Neuro-Oncology

Neuro-Oncology 18(7), 974–981, 2016
doi:10.1093/neuonc/nov318
Advance Access date 26 January 2016

Early treatment of HER2-amplified brain tumors with targeted NK-92 cells and focused ultrasound improves survival

Ryan Alkins, Alison Burgess, Robert Kerbel, Winfried S. Wels, and Kullervo Hynynen

Physical Sciences Platform, Sunnybrook Research Institute, Toronto, Ontario, Canada (R.A., A.B., K.H.); Medical Biophysics, University of Toronto, Toronto, Ontario, Canada (R.A., R.K., K.H.); Biological Sciences Platform, Sunnybrook Research Institute, Toronto, Ontario, Canada (R.K.); Georg-Speyer-Haus, Institute for Tumor Biology and Experimental Therapy, Frankfurt am Main, Germany (W.S.W.)

Corresponding Author: Ryan Alkins, MD, PhD, Sunnybrook Research Institute, 2075 Bayview Ave, C713, Toronto, ON M4N 3M5 (ryan.alkins@mail.utoronto.ca).

Background. Malignant brain tumors have a dismal prognosis, with residual tumor remaining after surgery necessitating adjuvant chemoradiotherapy. The blood-brain barrier hinders many chemotherapeutic agents, resulting in modest treatment efficacy. We previously demonstrated that targeted natural killer (NK)-92 cells could be delivered to desired regions of the brain using MRI-guided focused ultrasound and Definity microbubbles. Targeted NK-92 cells have advantages over many systemic therapies including their specific cytotoxicity to malignant cells (particularly those expressing the target antigen), ability to spare healthy cells, and being unaffected by efflux channels.

Methods. We investigated whether longitudinal treatments with targeted NK-92 cells, focused ultrasound, and microbubbles could slow tumor growth and improve survival in an orthotopic HER2-amplified rodent brain tumor model using a human breast cancer line as a prototype. The HER2 receptor, involved in cell growth and differentiation, is expressed by both primary and metastatic brain tumors. Breast cancers with HER2 amplification have a higher risk of CNS metastasis and poorer prognosis.

Results. Early intensive treatment with targeted NK-92 cells and ultrasound improved survival compared with biweekly treatments or either treatment alone. The intensive treatment paradigm resulted in long-term survival in 50% of subjects.

Conclusions. Many tumor proteins could be exploited for targeted therapy with the NK-92 cell line; combined with the mounting safety evidence for transcranial ultrasound, these results may soon be translatable to a highly targeted treatment option for patients with brain tumors.

Keywords: breast cancer, focused ultrasound, immune cell therapy, MRIgFUS.

Malignant brain tumors affect a large number of North Americans, with both primary and metastatic tumors having a dismal prognosis.[1–6] Macroscopic or microscopic residual tumor often remains after surgical resection, necessitating adjuvant chemo- and/or radiotherapy. Many chemotherapeutic agents are hindered by the blood-brain barrier (BBB). The BBB, which normally allows passage of only small lipophilic compounds into the CNS,[7] combined with efflux channels (expressed by both malignant and endothelial cells) acts to severely restrict the accumulation of many therapeutic agents in the brain.[8,9] Adjuvant therapies that successfully reach the brain often result in varying degrees of injury to healthy tissues, both intracranially and extracranially.[10] As a result, current intravenously delivered agents have modest efficacy in the treatment of brain tumors.

We have recently demonstrated that targeted natural killer (NK)-92 cells can be delivered to tumors in the brain using MRI-guided focused ultrasound (FUS) in combination with microbubble ultrasound contrast agents (Fig. 1).[11] Stable cavitation of microbubbles under the influence of submegahertz ultrasound frequencies temporarily alters the permeability of the cerebrovasculature in desired regions by disrupting endothelial tight junctions, increasing vesicular transport, and altering endothelial cell membrane proteins.[12–14] Additional cell-specific interactions, which are yet to be characterized, are also likely to be involved.[11] NK cells are cytotoxic lymphocytes involved in the innate immune response to malignant cells.[15] Targeted NK cells have advantages over other systemic therapies including specific cytotoxicity to malignant cells, which is heightened when encountering those malignant cells possessing the target

Received 18 April 2015; accepted 3 December 2015

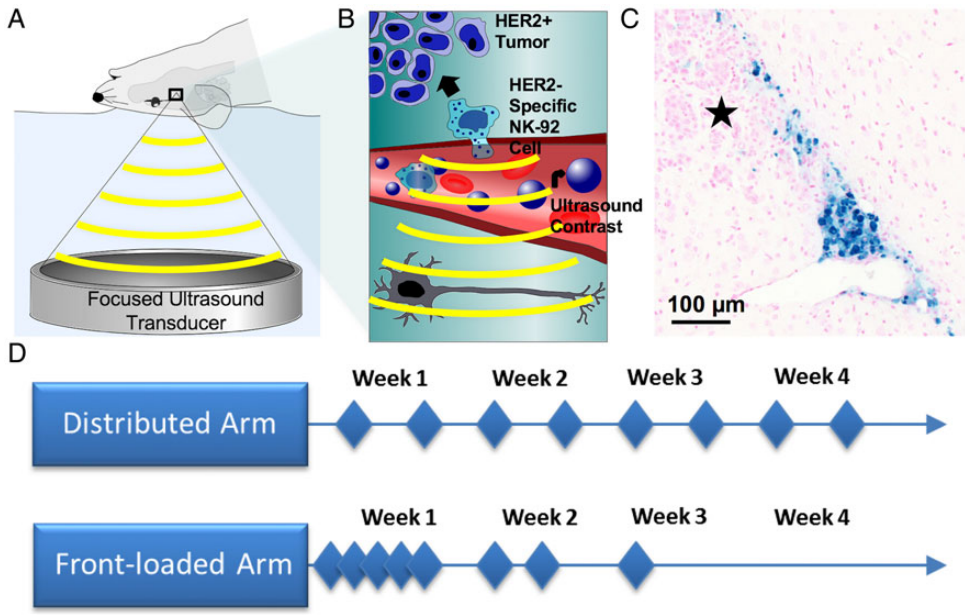

Fig. 1. A schematic representation of the treatment setup, effect, and organization of the study. (A) The focused ultrasound (FUS) treatment setup, with the focused transducer (551.5 kHz) coupled to the rodent via a bath of degassed water and targeted using MRI. (B) NK-92 cells extravasate from the cerebrovasculature following interaction with FUS and microbubbles at the site of the tumor 11. (C) NK-92 cells labeled with iron and stained with Prussian blue following FUS. The cells are tracking toward the tumor, denoted by the star (★). (D) The 2 treatment arms, with the diamonds each representing a treatment event. In each arm, animals were randomized to receive FUS+Cells, FUS, or Cells for the duration of the study.

antigen.[16] As such, once these cells gain access to the CNS, they appear to track to their target without appreciable impact on nontumor tissue.[1]

Many tumors express proteins that could be exploited for targeted cellular therapies. One such candidate is the human epithelial growth factor receptor (HER2) thought to be involved in signaling pathways regulating cell growth and differentiation and expressed by a number of epithelial tumors including breast and glioblastoma.[17,18] Breast cancers with HER2 amplification are more aggressive and have a higher risk of CNS metastasis and poorer prognosis.[17,19] Antibodies targeted to HER2 have resulted in improved tumor control and survival in HER2-amplified breast cancers but (along with NK cells) do not normally cross the BBB.[7,9] The HER2-specific NK-92-scFv(FRP5)-zeta cell line is a human NK-92 cell line modified to express a chimeric HER2 antigen receptor.[16] It has been shown to localize to both extracranial and, in conjunction with FUS, intracranial HER2-amplified tumors to cause selective tumor cell death.[11,16,20] The targeted NK-92 cell line has distinct advantages over direct antibodies to HER2 as it maintains cytotoxicity to HER2-negative tumor subpopulations. It also has advantages over systemic chemotherapy regimens and whole-brain radiation because it spares nonmalignant cells.

We hypothesized that multiple combined treatments of intravenously delivered HER2-specific NK-92 cells and FUS with microbubbles might control tumor growth and improve survival in a xenograft HER2-amplified brain metastasis model using a human metastatic breast cancer cell line as a prototype. With the recent demonstration of safe blood-brain barrier disruption (BBBD) with FUS in nonhuman primates,[21] clinical translation of the results may be possible in the not-too-distant future.

Materials and Methods

Study Design

This was a prospective, randomized, blinded study in athymic nude rats to determine if targeted NK-92 cells delivered to the brain could prolong survival in a HER2-amplified breast metastasis model. All procedures were approved by the Sunnybrook Research Institute Animal Care and Use Committee and conformed to the guidelines set out by the Canadian Council on Animal Care.

Cell Lines and Tumor Implantation

Human HER2-expressing MDA-MB-231 breast tumor cells were isolated from brain metastases as previously reported and transfected to express high levels of the HER2 receptor.[22] HER2 expression was confirmed by immunocytochemistry with primary rabbit anti-HER2 (Thermo Fisher Scientific). For tumor implantation, MDA-MB-231-HER2 cells were combined with BD Matrigel (BD Biosciences) at a density of 10^3 cells/μL, and 5 μL were injected stereotactically into the right frontal striatum of 200–250 g male athymic nude rats (Charles River Laboratories). Treatments began exactly 1 week following cell implantation.

The human cell line, NK-92 (ATCC), was virally transduced to stably express a chimeric antigen receptor specific to HER2.[16] The antigen receptor expression was confirmed by fluorescence-activated cell sorter analysis. Expression of CD45 was evaluated on a smear using mouse anti-human CD45 (R&D Systems). HER2-specific NK-92-scFv(FRP5)-zeta cells were maintained in X-VIVO 10 medium (Lonza) supplemented with 5% heat-inactivated human serum (Cedarlane), 0.6 mg/mL

G418 (Wisent), and 100 μg/mL IL-2 (R&D Systems). Cells were collected, centrifuged, and resuspended in sterile physiological saline at a concentration of 10^7 cells/mL for injection in vivo.

Treatment Arms

Thirty-one animals underwent 8 treatment sessions and were entered into 1 of 2 arms, each with a different schedule. Within each arm, animals were randomly assigned to receive combined FUS and targeted NK-92 cells (FUS + Cells), FUS alone (FUS), or cells alone (Cells). Cell injection consisted of i.v. injection of 10^9 targeted NK-92 cells/m^2 body surface area (estimated from body weight) on the order of the number of cells delivered in previous phase 1/2 trials. The first arm (distributed) received treatments twice per week for 4 weeks (Fig. 1D; FUS+Cells $N = 7$, FUS $N = 7$, Cells $N = 6$). The second arm (front-loaded) received 5 treatments in the first week, 2 treatments in the second week, and 1 treatment in the third week (Fig. 1; FUS + Cells $N = 4$, FUS $N = 3$, Cells $N = 4$). The order in which animals were treated at each of the 8 sessions was randomly assigned.

MRI-guided Focused Ultrasound

Definity ultrasound contrast (Lantheus Medical Imaging) was activated at room temperature with the VIALMIX (Lantheus) agitator, diluted 1:10 in 0.9% saline, and a 20 μL/kg dose was injected with the onset of sonication. Animals were positioned supine on an in-house–fabricated sled and transferred between the 7T MRI and an ultrasound system. The latter consisted of a 551.5 kHz single-element focused ultrasound transducer ($F = 0.8$, $R = 10$ cm) submerged in a bath of degassed water and combined with a 3-axis positioning system. The focal spot size for the transducer, characterized by the full-width at half maximum of the beam pressure profile, corresponded to a diameter of 3.0 mm in the axial plane by 12.5 mm in the beam direction. BBBD was performed (10 ms pulses, 2 Hz pulse repetition frequency, 120 s total duration) using a controller to monitor acoustic emissions and modulate acoustic power to predetermined ultraharmonic signatures.[23] The power was increased incrementally until this threshold was reached and then decreased to 60% of peak power for the remaining duration of sonication (which we had previously found to result in successful translocation of NK-92 cells into the CNS).[11]

All imaging was performed with a 7 T MRI (BioSpec 70/30 USR, Bruker BioSpin) fitted with gradient and shim inserts (BGA-S, Bruker BioSpin). MR imaging consisted of T2-weighted (TR = 3000 ms, TE = 37.2 ms, flip angle = 180°) and T1-weighted sequences (TR = 500 ms, TE = 10 ms) enhanced with a gadolinium contrast agent (0.2 mL/kg; Omniscan, GE Healthcare) in at least 2 perpendicular planes for treatment planning, estimation of tumor volume, and quantification of BBBD. Follow-up imaging performed beyond the treatment period consisted of axial and coronal proton-weighted MRI twice weekly.

Criteria for Study Exit

Animals were euthanized by euthanyl injection when they showed signs of pain, distress, or when their tumor dimensions or midline shift exceeded predetermined threshold values. Animals were monitored on a daily basis by veterinary technicians blinded to the study groups. They were also assessed and weighed by study personnel at the beginning of each treatment day prior to imaging. Signs of distress were defined as weight loss >20% in 1 week, lethargy, failure to groom, or the presence of neurological deficits. Tumor dimensions were followed with serial imaging, and a maximal tumor diameter of 10 mm, and/or midline shift >2 mm were taken as cutoffs for euthanasia. This was consistent with previous studies in which animals harboring tumors greater than these thresholds become rapidly symptomatic.[24]

Histological Analysis

The brain was removed following euthanasia, fixed in 10% neutral buffered formalin, and sectioned in 4 μm coronal sections cut at 250 μm levels. Histological analysis was blinded. A section at each level was stained with hematoxylin and eosin (H&E) for morphological analysis. At each level, a section was also stained for CD45 to survey for remaining HER2-specific NK-92 cells. Immunohistochemistry (IHC) using the polymerized reporter-enzyme staining system (Vector Laboratories) was used to detect CD45 (mouse anti-human, 1:200, R&D Systems). Sections containing the tumor were also stained for HER2 (rabbit anti-human HER2, Thermo Fisher Scientific) to examine whether the HER2-specific NK-92 changed or eradicated the HER2-amplified tumor populations. Sections were digitized with a Mirax Scanner (Zeiss) and analyzed using Pannoramic Viewer (v.1.15, 3DHISTECH).

Statistical Analysis

Graph Pad Prism 6 (Graph Pad Software) was used for statistical analysis. The enhancement data were analyzed using the Student *t* test. Survival data were compared using the Kaplan-Meier method with log-rank test. The average survival ± standard deviation for each group was also tabulated, and these were compared using 1-way ANOVA and Tukey post test. Statistical significance was noted if $P < .05$.

Results

Cytolytic activity of the targeted NK-92 cell line was confirmed by flow cytometry. Cell lysis was proportional to the ratio of effector-to-target cells, consistent with both previously published findings and our own prior results.[11,16] The success rate for tumor establishment was 100%, and progression was rapid as quantitatively assessed by serial MRI (Fig. 3A and E). For both treatment arms, the contrast enhancement on T1 MRI following BBBD was not statistically different between the FUS and FUS+Cells groups (distributed arm, $P = .10$; front-loaded arm, $P = .76$). Representative pre- and post-BBBD images are shown in Fig. 2.

Tumor Surveillance

Tumors began to cause severe mass effect with brain distortion and surrounding vasogenic edema at sizes nearing that preestablished for euthanization. The ipsilateral frontal horn of the lateral ventricle showed progressive effacement, with relative enlargement of the remaining ventricular system. Solid growth was seen initially, but cystic components developed after 2–3 weeks as seen on serial MRI (Fig. 3A and E) and

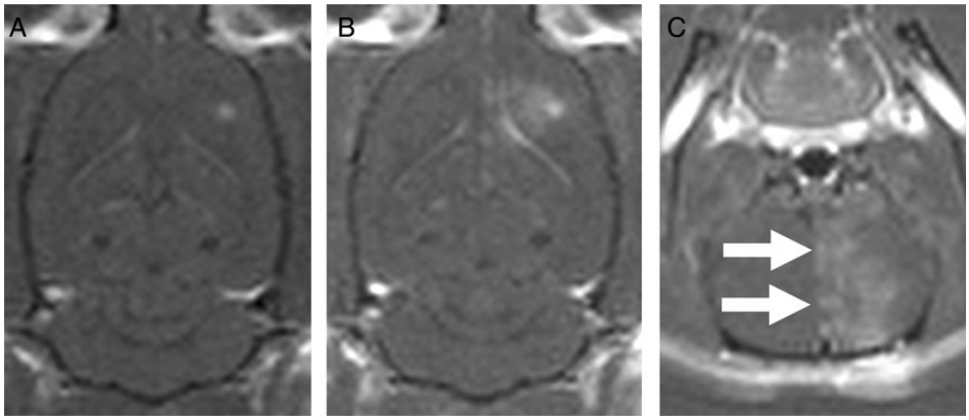

Fig. 2. Representative images of blood-brain barrier disruption (BBBD). The contrast enhancement in the tumor before (A) and after BBBD (B and C) are shown. The focus is larger than the tumor size, so increased permeability is seen in the peritumoral area, favoring the medial aspect of the tumor due to the curvature of the rat skull. The coronal image (C) shows heterogeneity in the enhancement pattern due to standing waves. There was no difference in the enhancement after BBBD between the focused ultrasound (FUS) and FUS+Cells groups in either arm.

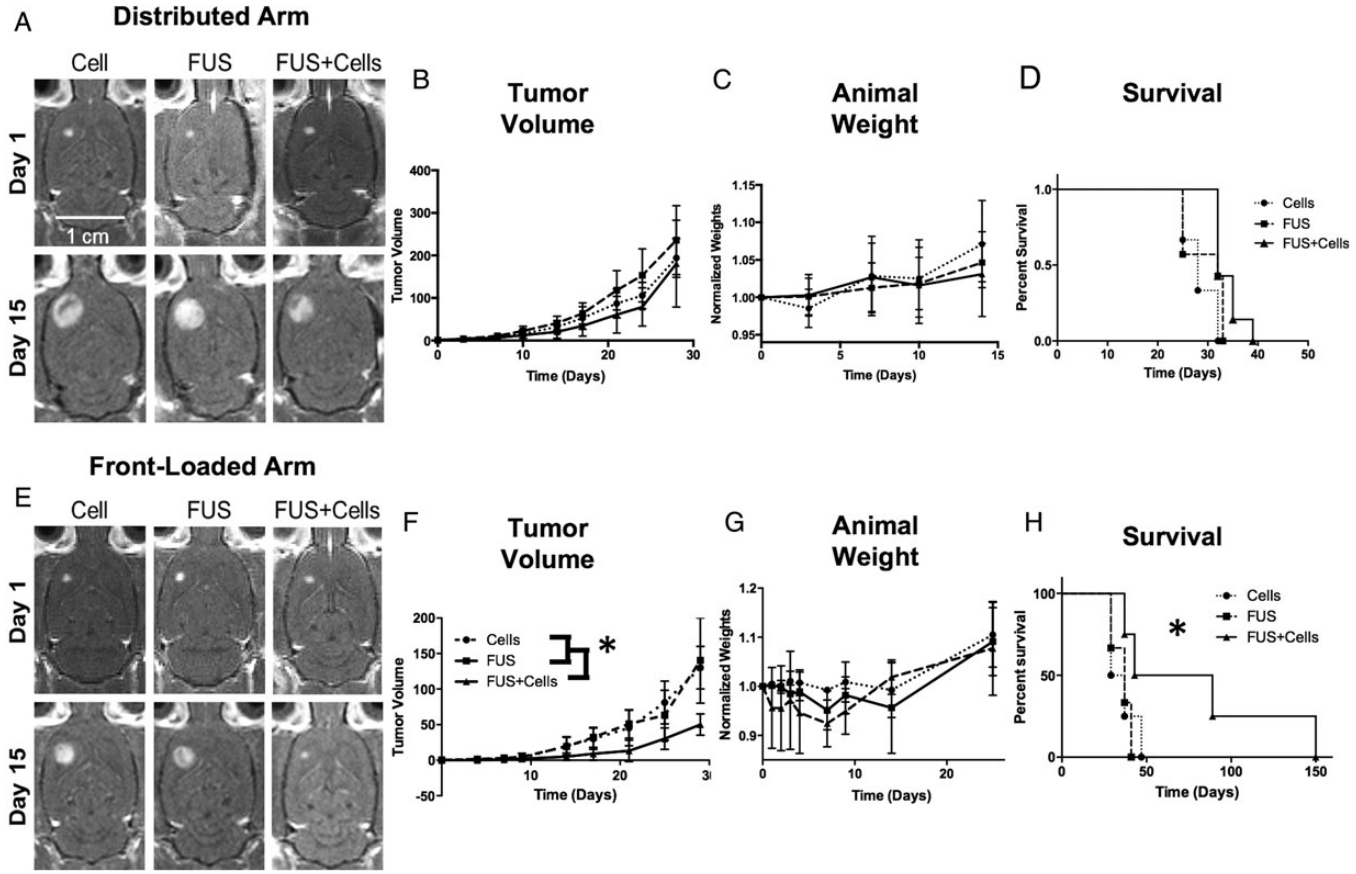

Fig. 3. Comparison of the distributed and front-loaded treatment arms. A and E are representative contrast-enhanced T1 MR images of the tumor progression at 14 days. (B–D) The tumor volumes, animal weights, and survival data for the distributed arm. (F–H) Same data for front-loaded arm. F and H show significant reduction in tumor volume and increase in survival, respectively, achieved with an aggressive treatment schedule. (G) The front-loaded schedule was taxing on the animals. An initial weight loss was measured in the animals, whereas this was not observed in the distributed arm. Statistically significant results are denoted by *.

were subsequently confirmed on histological examination (Fig. 5A and C). All animals except for one met the criteria for euthanasia based on size or mass effect rather than the appearance of behavioral symptoms.

The long-term survivors in the front-loaded arm were followed with MRI (Fig. 4) and did not show any evidence of tumor progression. A decrease in the volume of the frontal lobe in the region of the tumor was observed, as suggested by the prominence of the ipsilateral ventricle. It was impossible to distinguish whether this tissue loss was due to tumor or treatment or a combination of the two. The animal depicted in Fig. 4B had a more prominent "inflammatory" reaction surrounding the tumor, with significant peritumoral edema on MR imaging that occurred after the end of BBBD treatments and resolved spontaneously (but with more ensuing atrophy).

Tumor Progression

In the distributed arm, Kaplan-Meier analysis revealed a significant trend with $P = .075$. Tumor volumes in the FUS+Cells group appeared to have a slower growth rate initially, but this was not statistically different from the other groups; the volumes were nearly equivalent at the end of 4 weeks of treatment (Fig. 3B and D).

The front-loaded treatment arm was much more promising, with the Kaplan-Meier analysis (Fig. 3H) revealing a significant prolongation of survival in the FUS+Cells group compared with the other cohorts. There was also a statistically significant increase in the mean survival time for the FUS+Cells group of the front-loaded arm compared with the remaining groups in both arms ($P < .05$). There was no difference in survival between the FUS or Cells groups. The mean tumor volumes (measured at 28 days) were also significantly reduced in the FUS+Cells group of the front-loaded arm compared with the FUS or Cell groups ($30 \pm 57\ mm^3$ vs $93 \pm 53\ mm^3$; $P < .05$; Fig. 3F). The long-term survivors in the FUS + Cells group of the front-loaded arm showed no adverse effects up to the time of sacrifice, which was chosen to be 150 days.

The front-loaded treatment regimen was intensive and stressful for the animals and resulted in an arrest in weight gain for the Cell group and a weight loss in the 2 groups receiving ultrasound and BBBD (Fig. 3G). However, no animal had an adverse event related to the treatment schedule, and by 14 days all animals demonstrated parallel increasing growth trajectories. Similar to what was seen in the distributed arm (but to a lesser extent), approximately half of the animals in the FUS+Cells group appeared to have little response to the treatment, with survival times similar to the animals in the FUS and Cell alone groups.

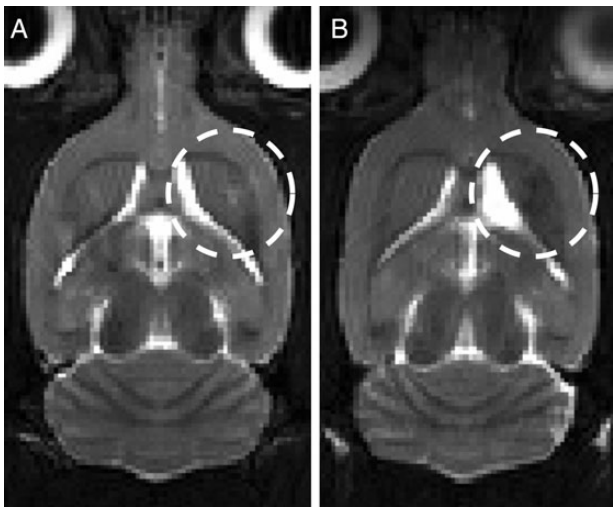

Fig. 4. Representative T2-weighted 7T MR images of the long-term survivors in the focused ultrasound (FUS) + Cells group of the front-loaded arm. The tumor location is indicated by the hashed circle. There is some signal heterogeneity in the frontal striatum and some tissue loss suggested by the increased prominence of the right frontal horn of the lateral ventricle. There were no blood products seen on postmortem examination to explain the MR signal. It is impossible to distinguish whether the atrophy was due to the treatment or the tumor. The long-term survivors were completely asymptomatic until the end of the study.

Histological Analysis

There were no signs of hemorrhage or erythrocyte extravasation on H&E staining within the tumor itself or the surrounding brain; however, most animals were euthanized a week or more after the last sonication (Fig. 5A–C, G, and H). Despite the differences in survival times for the animals depicted in Fig. 5A–C, the appearance of the tumor at the time of sacrifice was similar, suggesting that our study exit criteria were relatively robust. Many of the tumors developed large cystic components that were initially identifiable on MRI surveillance. IHC for CD45 at the time of animal sacrifice did not reveal any surviving targeted NK-92 cells in the brain (Fig. 5I). Despite confirming the parent tumor cell line to be 90% positive for HER2 by IHC prior to tumor implantation, there was heterogeneous expression in both treatment arms on postmortem examination, which was not entirely explained by treatment group (Fig. 5D–F). In some cases, it did appear that the treated tumor volume contained a paucity of HER2 expression compared with the untreated tumor volume (Fig. 5E and F).

Discussion

In the present study, we had a positive impact on survival when both targeted NK-92 cells and FUS were combined early during the course of tumor development (front-loaded arm) but were unsuccessful at achieving any appreciable effect on tumor progression with FUS or NK-92 cells on their own. Later treatments in the distributed arm, once tumors reached moderate volume, appeared to be as ineffective as the control treatments. As such, the treatment described might be most effective when combined with a cytoreductive procedure such as surgical resection or ablation, which could be accomplished in the same setting to exploit the thermal mechanisms of ultrasound.[25,26] The combined treatment effect of focused ultrasound, microbubbles, and targeted NK-92 cells was not uniform in the front-loaded arm, where roughly half of the animals experienced a treatment failure relatively early on. This could be appreciated to a lesser extent even in the distributed arm. Interestingly, a similar phenomenon has been observed in other

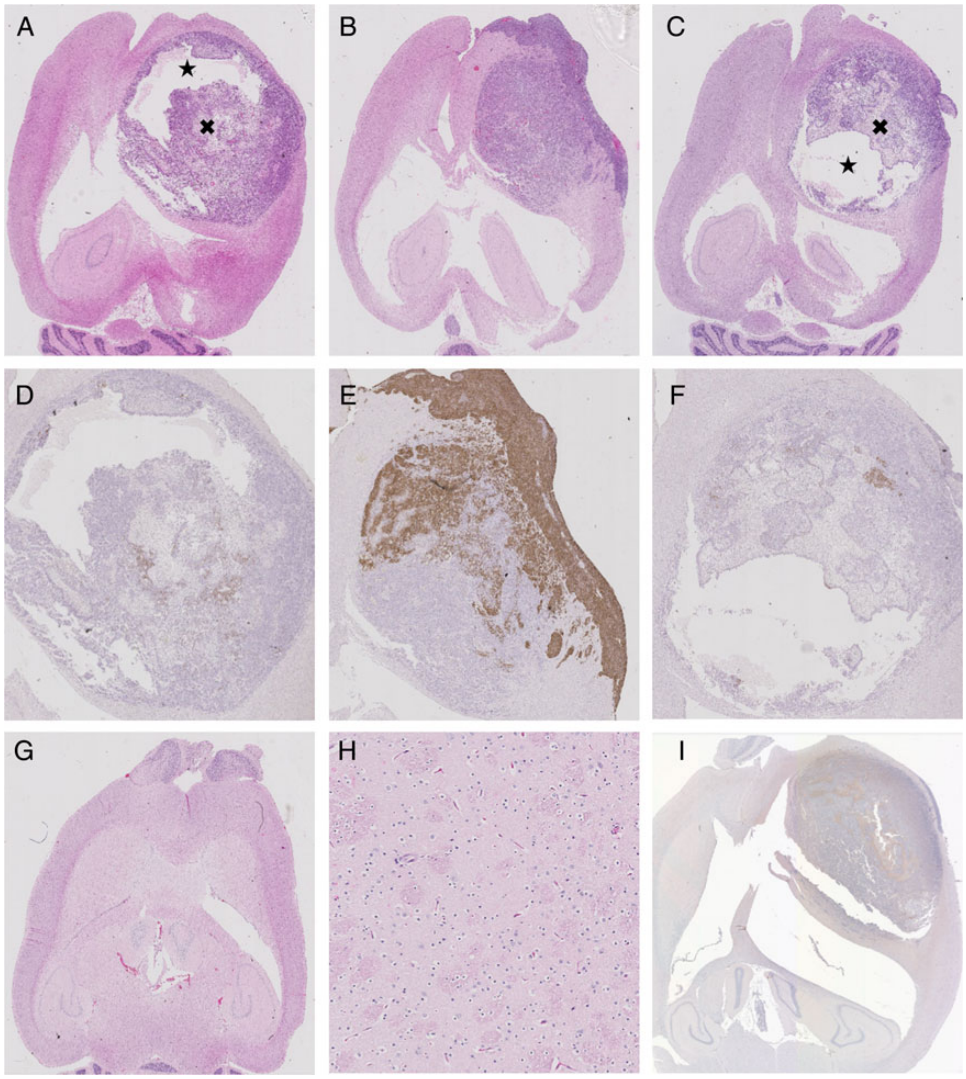

Fig. 5. Histopathological results depicting tumor progression and cell populations in the front-loaded arm. A–C depict H&E stained sections in the focused ultrasound (FUS) + Cells group (A) and (B) and the Cell group (C). The corresponding higher magnification images of HER2 expression are shown in D–F. The cystic (★) and necrotic (×) regions are identified in A and C, preventing NK-92 cells from circulating through and accumulating in parts of the tumor. There are virtually no HER2-positive cells in D, suggesting that this subpopulation was wiped out by the targeted NK-92 cells. Furthermore, in E, the leptomeningeal disease and the portion of the tumor closest to the skull were more uniformly HER2-positive; these areas were somewhat sheltered from the FUS treatment due to lensing effects of the rodent skull. The tumor farthest from the skull, more readily targeted by the FUS, is again void of HER2-positive cells. There was some variability of HER2 expression even in the Cell group (F), where we didn't expect the targeted NK-92 cells to have any effect. Representative H&E of one of the long-term survivors (G), with a high-magnification view of the tumor region in H (field of view 88 μm). The ventricular prominence can again be seen (G) without any evidence of hemorrhage or residual tumor (G, H). Representative CD-45 staining, showing no evidence of NK-92 cells remaining at the time of sacrifice (I).

studies of FUS and brain tumors in which 2 distinct groups emerged: 1 with a promising response to the therapy and the other behaving similarly to the controls.[24]

These failures are unlikely to represent more resistant tumor phenotypes, given that all the tumors were derived from the same parent cell line. We postulate that these difficulties were in part associated with scaling BBBD to the rodent. Our results suggest that FUS+Cells are more effective when delivered to animals with a small tumor burden, so that an early ineffective treatment would have a more pronounced effect. At ultrasound frequencies in the half-megahertz range, with the current transducer and rat skull geometry, standing waves have been detected in up to 25% of animals despite a low-duty cycle pulse sequence (Fig. 2C).[27] Large aperture hemispherical arrays are used in humans, in addition to a low-duty cycle, to reduce the occurrence of standing waves but are difficult to implement in rodent models. Furthermore, in humans the distance of the focus from any rigid boundary is much greater, as is the ratio of the internal dimensions of the skull to the wavelength, making the conditions for standing wave effects less favorable. In a rodent model, much or even the entire tumor could be near a node, significantly reducing the treated

volume. If this occurred early in the treatment when the tumors were small, the entire tumor could have been undertreated or untreated, compromising the therapeutic response. Even in larger tumors the effects of standing waves would negatively affect the delivery of cells.

Further size-dependent effects include the recruitment of NK-92 cells from within the sonicated region situated outside of the tumor. The sonicated volume encompassed proportionally more normal brain when the tumors were small, which may act as somewhat of a reservoir for cells that can be recruited to the tumor site (as we had observed in our previous study).[11] A further issue related to the small size of the rodent skull and the lack of a multi-element hemispherical array is the lensing effect that can occur when the incident ultrasound wave is not orthogonal to the skull. This would bias the focus toward the midline in our setup and possibly miss portions of the tumor closer to the skull (Figs. 2A and 5E). Additional factors that may have reduced treatment efficacy include the development of cystic compartments and necrosis, both of which negatively affect vascular access to the tumor.

Consistent with work previously published using the HER2-specific NK-92-scFv(FRP5)-zeta cell line, we found the killing efficiency increased proportionally with the ratio of effector-to-target cells.[11,16] Extending these in vitro results to the in vivo scenario, it is likely that as tumors got progressively larger, and the delivery of targeted NK-92 cells became more variable, a decreasing ratio of targeted NK-92-to-tumor cells contributed to the waning efficacy of the treatment. Given that NK-92 cells do not persist long in the absence of IL-2,[28] it is also not surprising that none were seen on postmortem examination. Most animals were examined more than a week after the last injection of NK-92 cells, much longer the cells would be expected to survive without supplemental IL-2. We postulate that the front-loaded group effectively achieved an effector-to-tumor cell ratio that resulted in appreciable killing, as the daily treatments allowed NK-92 cells to accumulate within the tumor, while the interval time for tumor growth compared with the distributed arm was much shorter. In the distributed arm, most NK-92 cells from the previous treatment would not have been viable by the time of subsequent treatment, and the tumor would have also had more interval growth. Concerns have previously been raised in the literature about the possibility of an unabated clonal expansion of NK-92 cells, but we did not detect any clinical evidence of this in the brain, nor did it impact the endpoints in the current study.

The tumor cell line used in our study was known from our previous work to be ~90% positive for HER2. In some Cell animals, where we expected virtually no targeted NK-92 and thus no selective pressure on HER2-positive cell proliferation, the tumor was predominantly HER2-negative by the time it was examined histologically (Fig. 5F). On the other hand, in some cases it appeared as though the treated regions harbored fewer HER2-positive tumor cells, and those areas not accessible to ultrasound expressed the protein more uniformly. In 1 of the 2 FUS+Cells animals that died early on, leptomeningeal disease was seen on histological assessment (Fig. 5E). Interestingly, this region of tumor was much more uniformly HER-positive compared with the parenchymal component that was targeted by the ultrasound; however, it is difficult to draw any more concrete conclusions given that this was only seen in a single animal. Regardless, despite verifying that a high percentage of cells overexpressed HER2 at the onset of experiments, the population evolved with considerable variability. In the same vein, the HER2-negative subpopulation did not lead to treatment-resistant HER2-negative tumor as evidenced by the 50% long-term survival in the front-loaded arm. This may be explained by the fact that the HER2-specific NK-92 cells maintained cytotoxicity toward HER2-negative tumor cells as well—albeit with less affinity—so if they managed to reach the tumor, they had effectively lysed HER2-negative cells. Furthermore, if it is accepted that treatment is most effective when the tumor burden is small, as our data suggest, by the time most tumors were analyzed they would have been growing unabated for weeks; therefore, any changes might have been obscured.

We have demonstrated the tumor control and survival advantages achieved using targeted immune cells combined with MRI-guided FUS and microbubbles. Our results suggest that multiple treatments early in the course of tumor development are necessary when using the current technique in order to obtain efficacious effector-to-tumor ratios. This pilot study was limited by its small sample size and the use of only a single tumor cell line, owing to the highly resource-intensive nature of these experiments. Another limitation was scaling the FUS to the rodent skull geometry. Future work might include optimization of effector cell delivery, both in overall numbers and increased spatial uniformity. Other optimizations might involve the concomitant administration of systemic IL-2 to prolong viability of the NK-92 cells. We have reluctantly referred to the FUS treatments as BBBD, as there was little question that the cerebrovasculature was made more permeable to gadolinium contrast. The FUS-NK-92 cell transmigration mechanism, however, may have more to do with interactions at the endothelial cell membrane rather than disruption of tight junctions. For example, Caveolin-1 is upregulated after FUS and is also implicated in diapedesis.[14,29] The exact mechanisms remain unknown, but elucidating them could be valuable for optimizing the current therapy.

Funding

This research was funded by the National Institutes of Health (R01 EB003268 to K.H.), the Weston Foundation and the Canada Research Chair Program. Alison Burgess was partially funded by a Heart and Stroke Foundation of Canada fellowship.

Acknowledgments

We would like to thank Shawna Rideout-Gros and Alexandria Garces for their assistance with the experiments.

Conflict of interest statement. None declared.

References

1. Nussbaum ES, Djalilian HR, Cho KH, Hall WA. Brain metastases. Histology, multiplicity, surgery, and survival. *Cancer*. 1996;78(8):1781–1788.

2. Hall WA, Djalilian HR, Nussbaum ES, Cho KH. Long-term survival with metastatic cancer to the brain. *Med Oncol*. 2000;17(4): 279–286.
3. Ohgaki H, Dessen P, Jourde B, et al. Genetic pathways to glioblastoma: a population-based study. *Cancer Res*. 2004; 64(19):6892–6899.
4. Stupp R, Mason WP, van den Bent MJ, et al. Radiotherapy plus concomitant and adjuvant temozolomide for glioblastoma. *N Engl J Med*. 2005;352(10):987–996.
5. Miralbell R, Mornex F, Greiner R, et al. Accelerated radiotherapy, carbogen, and nicotinamide in glioblastoma multiforme: report of European Organization for Research and Treatment of Cancer trial 22933. *J Clin Oncol*. 1999;17(10):3143–3149.
6. Patchell RA. The management of brain metastases. *Cancer Treat Rev*. 2003;29(6):533–540.
7. Abbott NJ, Ronnback L, Hansson E. Astrocyte-endothelial interactions at the blood-brain barrier. *Nat Rev Neurosci*. 2006; 7(1):41–53.
8. Muldoon LL, Soussain C, Jahnke K, et al. Chemotherapy delivery issues in central nervous system malignancy: a reality check. *J Clin Oncol*. 2007;25(16):2295–2305.
9. Pardridge WM. The blood-brain barrier: bottleneck in brain drug development. *NeuroRx*. 2005;2(1):3–14.
10. Kannarkat G, Lasher EE, Schiff D. Neurologic complications of chemotherapy agents. *Curr Opin Neurol*. 2007;20(6):719–725.
11. Alkins R, Burgess A, Ganguly M, et al. Focused ultrasound delivers targeted immune cells to metastatic brain tumors. *Cancer Res*. 2013;73(6):1892–1899.
12. Sheikov N, McDannold N, Sharma S, Hynynen K. Effect of focused ultrasound applied with an ultrasound contrast agent on the tight junctional integrity of the brain microvascular endothelium. *Ultrasound Med Biol*. 2008;34(7):1093–1104.
13. Sheikov N, McDannold N, Vykhodtseva N, Jolesz F, Hynynen K. Cellular mechanisms of the blood-brain barrier opening induced by ultrasound in presence of microbubbles. *Ultrasound Med Biol*. 2004;30(7):979–989.
14. Deng J, Huang Q, Wang F, et al. The role of caveolin-1 in blood-brain barrier disruption induced by focused ultrasound combined with microbubbles. *J Mol Neurosci*. 2012;46(3): 677–687.
15. Smyth MJ, Hayakawa Y, Takeda K, Yagita H. New aspects of natural-killer-cell surveillance and therapy of cancer. *Nat Rev Cancer*. 2002;2(11):850–861.
16. Uherek C, Tonn T, Uherek B, et al. Retargeting of natural killer-cell cytolytic activity to ErbB2-expressing cancer cells results in efficient and selective tumor cell destruction. *Blood*. 2002; 100(4):1265–1273.
17. Slamon DJ, Clark GM, Wong SG, Levin WJ, Ullrich A, McGuire WL. Human breast cancer: correlation of relapse and survival with amplification of the HER-2/neu oncogene. *Science*. 1987; 235(4785):177–182.
18. Mineo JF, Bordron A, Baroncini M, et al. Low HER2-expressing glioblastomas are more often secondary to anaplastic transformation of low-grade glioma. *J Neurooncol*. 2007;85(3): 281–287.
19. Lin NU, Bellon JR, Winer EP. CNS metastases in breast cancer. *J Clin Oncol*. 2004;22(17):3608–3617.
20. Daldrup-Link HE, Meier R, Rudelius M, et al. In vivo tracking of genetically engineered, anti-HER2/neu directed natural killer cells to HER2/neu positive mammary tumors with magnetic resonance imaging. *Eur Radiol*. 2005;15(1):4–13.
21. McDannold N, Arvanitis CD, Vykhodtseva N, Livingstone MS. Temporary disruption of the blood-brain barrier by use of ultrasound and microbubbles: safety and efficacy evaluation in rhesus macaques. *Cancer Res*. 2012;72(14):3652–3663.
22. Francia G, Man S, Lee CJ, et al. Comparative impact of trastuzumab and cyclophosphamide on HER-2-positive human breast cancer xenografts. *Clin Cancer Res*. 2009;15(20):6358–6366.
23. O'Reilly MA, Hynynen K. Blood-brain barrier: real-time feedback-controlled focused ultrasound disruption by using an acoustic emissions-based controller. *Radiology*. 2012;263(1):96–106.
24. Park EJ, Zhang YZ, Vykhodtseva N, McDannold N. Ultrasound-mediated blood-brain/blood-tumor barrier disruption improves outcomes with trastuzumab in a breast cancer brain metastasis model. *J Control Release*. 2012;163(3):277–284.
25. McDannold N, Clement GT, Black P, Jolesz F, Hynynen K. Transcranial magnetic resonance imaging- guided focused ultrasound surgery of brain tumors: initial findings in 3 patients. *Neurosurgery*. 2010;66(2):323,32; discussion 332.
26. Ram Z, Cohen ZR, Harnof S, et al. Magnetic resonance imaging-guided, high-intensity focused ultrasound for brain tumor therapy. *Neurosurgery*. 2006;59(5):949,55; discussion 955–6.
27. O'Reilly MA, Huang Y, Hynynen K. The impact of standing wave effects on transcranial focused ultrasound disruption of the blood-brain barrier in a rat model. *Phys Med Biol*. 2010;55(18): 5251–5267.
28. Gong JH, Maki G, Klingemann HG. Characterization of a human cell line (NK-92) with phenotypical and functional characteristics of activated natural killer cells. *Leukemia*. 1994;8(4):652–658.
29. Millan J, Hewlett L, Glyn M, Toomre D, Clark P, Ridley AJ. Lymphocyte transcellular migration occurs through recruitment of endothelial ICAM-1 to caveola- and F-actin-rich domains. *Nat Cell Biol*. 2006;8(2):113–123.